



## Phase switching in a voltage-biased Aharonov-Bohm interferometer

Vadim I. Puller<sup>1</sup> and Yigal Meir<sup>1,2</sup>

<sup>1</sup>*Department of Physics, Ben-Gurion University of the Negev, Beer Sheva 84105, Israel*

<sup>2</sup>*The Ilse Katz Center for Meso- and Nano-scale Science and Technology, Ben-Gurion University, Beer Sheva 84105, Israel*

(Received 12 December 2007; revised manuscript received 24 February 2008; published 18 April 2008)

A recent experiment [M. Sigrist *et al.*, Phys. Rev. Lett. **98**, 036805 (2007)] reported switches between 0 and  $\pi$  in the phase of Aharonov-Bohm (AB) oscillations of the two-terminal differential conductance through a two-dot ring with increasing voltage bias. Using a simple model, where one of the dots contains multiple interacting levels, these findings are explained as a result of transport through the interferometer being dominated at different biases by quantum dot levels of different “parities” (i.e., the sign of the overlap integral between the dot state and the states in the leads). The redistribution of electron population between different levels with bias leads to the fact that the number of switching events is not necessarily equal to the number of dot levels, in agreement with experiment. For the same reason, switching does not always imply that the parity of levels is strictly alternating. Lastly, it is demonstrated that the correlation between the first switching of the phase and the onset of the inelastic cotunneling, as well as the sharp (rather than gradual) change of phase when switching occurs, give reason to think that the present interpretation of the experiment is preferable to the one based on electrostatic AB effect.

DOI: [10.1103/PhysRevB.77.165421](https://doi.org/10.1103/PhysRevB.77.165421)

PACS number(s): 73.23.-b, 73.23.Hk, 73.63.Kv

### I. INTRODUCTION

The phase of a transmission coefficient through a quantum dot (QD) can be experimentally studied using an Aharonov-Bohm (AB) interferometer with the QD embedded in one of its arms.<sup>1,2</sup> Since the early experiments,<sup>1</sup> a large body of theoretical work have been devoted to study of the rich phase behavior experimentally discovered. When studied in two-terminal geometry, such an interferometer exhibits “phase rigidity,” i.e., the AB oscillations of conductance have either maximum or minimum at zero magnetic field, which corresponds to a transmission phase equal to 0 or  $\pi$ . Phase rigidity has its origins in time-reversal symmetry (i.e., unitarity of the transmission matrix).<sup>3</sup> In “open” interferometers<sup>4</sup> or two-terminal interferometers in nonequilibrium conditions,<sup>5</sup> the phase rigidity may be broken, i.e., the phase may change continuously. Particularly interesting are phenomena connected to “phase lapses,” which are abrupt changes of the transmission phase as a function of the plunger voltage in the Coulomb blockade valley (i.e., between two successive Coulomb blockade resonances). While there has not been yet general agreement about the physics underlying this phenomenon,<sup>6–8</sup> it is believed to be the consequence of the system undergoing transitions between regimes where transport is dominated by different levels.<sup>6–9</sup>

Recently, an interesting new phase phenomenon has been observed<sup>10</sup> in an AB interferometer under nonequilibrium conditions (i.e., with finite bias applied between the source and the drain). In this experiment, the differential conductance of a two-terminal interferometer was measured as a function of the bias voltage and magnetic flux through the interferometer. Both arms of the interferometer contained quantum dots, which were tuned to the Coulomb blockade regime, thus allowing only for cotunneling transport. As a function of bias, several switches of the phase of the AB oscillations between the values 0 and  $\pi$  were observed with the first switch coinciding with the onset of inelastic cotunneling in one of the dots.

A possible explanation for this effect may be as the result of electrostatic AB oscillations, as was studied in Refs. 11 and 12. Some features of the experiment, however, are inconsistent with such an explanation. In particular, as mentioned above, there is apparent correlation between the onset of the phase switching and the onset of inelastic cotunneling. In addition, the phase of AB oscillation, which at finite bias is not limited by symmetry to 0 or  $\pi$ , is in fact, changing abruptly between these values as a function of bias, whereas in Ref. 12 it changed smoothly.

An alternative explanation (motivated by “population switching” studies)<sup>6,7,9</sup> is that, depending on the bias voltage, the elastic contribution to the transport through the quantum dot may be dominated by different orbital states within the dot. Depending on the sign of the matrix elements between the state in the dot and the states in the leads<sup>13</sup> (“parity” of the state), an electron can acquire phase 0 or  $\pi$ , additional to the other phases acquired when traversing the interferometer. This results in AB oscillations having maximum or minimum depending on the parity of the current-transmitting state. Thus, if the two adjacent QD states have different parities, the phase switching may occur in the regimes when the state dominating the coherent transport changes from one to the other, which may happen with increasing bias.

From the simple theory described above, one would naively expect that, if more than two levels in the dot are energetically accessible, multiple switching events would occur only when the levels have alternating parities, and the number of switching events would then be equal to the number of parity changes. This presumption contradicts the experiment where the number of switchings can, in fact, be greater than the number of inelastic onsets,<sup>10</sup> i.e., greater than the number of the QD levels involved. In what follows, we will show that neither of these expectations is quite true, and a simple model can reproduce all the features of the experiment<sup>10</sup> as a result of redistribution of electron population between QD states. We also point out that at finite bias, “population in-

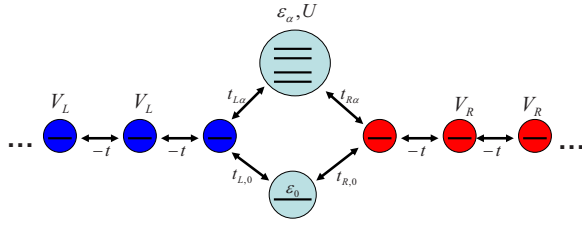


FIG. 1. (Color online) Schematic diagram of the modeled device. Two infinite tight-binding chains, possibly with different chemical potentials, are coupled to an Aharonov-Bohm interferometer, one of the arms of which contains a multilevel quantum dot.

version” is not a necessary condition for the phase switching to be observed.

The plan of this paper is as follows: In Sect. II, we first introduce our model of the interferometer, which, after a Schrieffer–Wolff (SW) transformation,<sup>14</sup> allows us to study cotunneling processes in terms of a single particle scattered from a local pseudospin degree of freedom. In Sec. III, this model is solved in terms of rate equations and the differential conductance is obtained as a function of the Aharonov-Bohm flux threading the interferometer and source-drain bias. We compare results with the experiment, showing, in particular, that the number of switching events can be greater or less than the number of levels, whose energy spacing is within the bias window. We discuss how the switching behavior may occur even when the parity of levels is not strictly alternating, and compare our results with the electrostatic AB scenario.

## II. MODEL

### A. Hamiltonian

We describe the interferometer by a tight-binding model, schematically shown in Fig. 1. The Coulomb interaction is present in one of the dots, which contains several electron orbitals (interacting arm), whereas the dot in the other arm of the interferometer (reference arm) has only one level. The chemical potential is set out of resonance, so that the transport via the interacting arm occur only by means of cotunneling processes. The reference arm can be characterized by its one-particle transmission coefficient, and placing a level in it is a matter of computational convenience.

In the present experimental context, the Kondo effect is irrelevant and its effects will be neglected in the present approach. In addition, for computational simplicity, we assume that each level carries a different quantum number, which are not mixed in the leads (i.e., we disregard difference between spin and orbital channels). The results obtained below can be shown to be correct also in the case when the number of channels in the leads is not equal to the number of states in the quantum dot (e.g., when all the levels in the dot are coupled to the same lead channel). However, since the dot levels in such a system are connected via tunneling into the leads, the correct calculation is more complicated and requires a decomposition procedure similar to that developed in Ref. 15.

Cotunneling processes can be described as second order transitions between different states which contain exactly one electron in the dot.<sup>16</sup> By performing a Schrieffer–Wolff transformation<sup>14</sup> (Appendix A), we can reduce the problem to that of one-particle scattered by local pseudospin degree of freedom. As a result, we can describe the system by the following (one-particle) Hamiltonian:

$$\mathcal{H} = H_L + H_R + H_D + W_{ref} + W_2 + W_4 + W_6, \quad (1)$$

where

$$H_L = \sum_{\alpha} \sum_{n=-\infty}^{-1} [V_L c_{\alpha,n}^+ c_{\alpha,n} - t(c_{\alpha,n-1}^+ c_{\alpha,n} + c_{\alpha,n}^+ c_{\alpha,n-1})], \quad (2a)$$

$$H_R = \sum_{\alpha} \sum_{n=1}^{+\infty} [V_R c_{\alpha,n}^+ c_{\alpha,n} - t(c_{\alpha,n+1}^+ c_{\alpha,n} + c_{\alpha,n}^+ c_{\alpha,n+1})], \quad (2b)$$

$$H_D = \sum_{\alpha} \epsilon_{\alpha} n_{\alpha}, \quad (2c)$$

$$W_{ref} = - \sum_{\alpha} (\omega_{rr} c_{\alpha,1}^+ c_{\alpha,1} + \omega_{lr} c_{\alpha,-1}^+ c_{\alpha,-1} + \omega_{rl} c_{\alpha,1}^+ c_{\alpha,-1} + \omega_{ll} c_{\alpha,-1}^+ c_{\alpha,-1}), \quad (2d)$$

$$W_2 = - \sum_{\alpha} (v_{rr}^{\alpha} c_{\alpha,1}^+ c_{\alpha,1} + v_{lr}^{\alpha} c_{\alpha,-1}^+ c_{\alpha,-1} + v_{rl}^{\alpha} c_{\alpha,1}^+ c_{\alpha,-1} + v_{ll}^{\alpha} c_{\alpha,-1}^+ c_{\alpha,-1}), \quad (2e)$$

$$W_4 = \sum_{\alpha, \beta \neq \alpha} (v_{rr}^{\beta\alpha} c_{\beta,1}^+ d_{\alpha}^+ d_{\beta} c_{\alpha,1} + v_{lr}^{\beta\alpha} c_{\beta,-1}^+ d_{\alpha}^+ d_{\beta} c_{\alpha,1} + \quad (2f)$$

$$v_{rl}^{\beta\alpha} c_{\beta,1}^+ d_{\alpha}^+ d_{\beta} c_{\alpha,-1} + v_{ll}^{\beta\alpha} c_{\beta,-1}^+ d_{\alpha}^+ d_{\beta} c_{\alpha,-1}), \quad (2g)$$

$$W_6 = - \sum_{\alpha, \beta \neq \alpha} (v_{rr}^{\alpha\alpha} n_{\beta} c_{\alpha,1}^+ c_{\alpha,1} + v_{lr}^{\alpha\alpha} n_{\beta} c_{\alpha,-1}^+ c_{\alpha,-1} + v_{rl}^{\alpha\alpha} n_{\beta} c_{\alpha,1}^+ c_{\alpha,-1} + v_{ll}^{\alpha\alpha} n_{\beta} c_{\alpha,-1}^+ c_{\alpha,-1}). \quad (2h)$$

with  $n_{\alpha} = d_{\alpha}^{\dagger} d_{\alpha}$ . Here,  $\alpha$  and  $\beta$  refer to the different dot levels and/or lead channels, whereas  $n$  is the tight-binding site label with  $n > 0$  ( $n < 0$ ) in the right (left) lead.  $c_{\alpha,n}^+$  ( $c_{\alpha,n}$ ) creates (annihilates) an electron in channel  $\alpha$  on site  $n$ , whereas  $d_{\alpha}^{\dagger}$  ( $d_{\alpha}$ ) creates (annihilates) electron in state  $\alpha$  in the quantum dot with energy  $\epsilon_{\alpha}$ .  $V_L$  and  $V_R$  are the potentials applied to the leads, related to the chemical potentials as  $\mu_{L,R} = \epsilon_F + V_{L,R}$  ( $\epsilon_F$  is the Fermi energy), and  $t$  is the hopping integral.

The terms  $H_L$  and  $H_R$  describe noninteracting leads,  $H_D$  is the Hamiltonian of the dot, and  $W_2$  and  $W_6$  describe elastic cotunneling through the quantum dot when it is empty or occupied by one electron, respectively.  $W_4$  describes inelastic cotunneling, i.e., the processes when an electron incident in channel  $\alpha$  is scattered into channel  $\beta$ , while the dot changes its state from  $\beta$  to  $\alpha$ .  $W_{ref}$  describes tunneling through the reference arm, which we have taken as channel independent.

The AB phase,  $\phi_{AB}$ , can be attached to the matrix elements for the reference arm:  $\omega_{rl} = \omega_{lr}^* = |\omega_{rl}| \exp(i\phi_{AB})$ . The explicit dependence of the tunneling parameters  $v$  and  $\omega$  on the original parameters appear in Appendix A.

### B. Scattering matrix

The energy of the system “QD+incident electron” is conserved, so we can start with calculating the scattering matrix, which we do by solving the Schrödinger equation,

$$\mathcal{H}|\Psi\rangle = E|\Psi\rangle, \quad (3)$$

where  $E$  is the energy of the system QD+incident electron, and the wave function can be written as

$$|\Psi\rangle = \sum_{\alpha,\beta} \left[ \sum_{n=-\infty}^{-1} (A_L^{\alpha\beta} e^{iq_\beta n} + B_L^{\alpha\beta} e^{-iq_\beta n}) d_{\beta}^+ c_{\alpha,n}^+ + \sum_{n=1}^{+\infty} (A_R^{\alpha\beta} e^{ik_\beta n} + B_R^{\alpha\beta} e^{-ik_\beta n}) d_{\beta}^+ c_{\alpha,n}^+ \right] |0\rangle, \quad (4)$$

where  $|0\rangle$  is the state with no particles. The wave vectors  $q_\beta$  and  $k_\beta$  are defined as solutions of the equations

$$E = \epsilon_\beta + V_L - 2t \cos q_\beta, \\ E = \epsilon_\beta + V_R - 2t \cos k_\beta \quad (5)$$

[ $\epsilon_L(q) = V_L + \epsilon_q$  and  $\epsilon_R(k) = V_R + \epsilon_k$ , where  $\epsilon_k = -2t \cos k$  are electron tight-binding eigenenergies in the two leads]. Let  $M$  be the number of the channels, then  $\mathbf{A}_L$ ,  $\mathbf{A}_R$ ,  $\mathbf{B}_L$ , and  $\mathbf{B}_R$  are vectors with  $M^2$  components and the amplitude scattering matrix can be defined as (more details are given in Appendix B)

$$\begin{pmatrix} \mathbf{B}_L \\ \mathbf{A}_R \end{pmatrix} = \hat{S} \begin{pmatrix} \mathbf{A}_L \\ \mathbf{B}_R \end{pmatrix}, \quad \hat{S} = \begin{pmatrix} \hat{S}_{LL} & \hat{S}_{LR} \\ \hat{S}_{RL} & \hat{S}_{RR} \end{pmatrix}. \quad (6)$$

In order to normalize the wave function and the scattering matrix to unit incident flux, we multiply  $\hat{S}$  by velocity matrices

$$\hat{S} = \hat{u}^{1/2} \hat{S} \hat{u}^{-1/2}, \quad \hat{u} = \begin{pmatrix} \hat{u}_L & 0 \\ 0 & \hat{u}_R \end{pmatrix}, \quad (7)$$

where

$$u_L^{\alpha,\beta;\alpha'\beta'} = \delta_{\alpha,\alpha'} \delta_{\beta,\beta'} 2t \sin q_\beta, \\ u_R^{\alpha,\beta;\alpha'\beta'} = \delta_{\alpha,\alpha'} \delta_{\beta,\beta'} 2t \sin k_\beta. \quad (8)$$

### C. Transition rates

In order to get the rate equations, we write down the rate at which electrons incident from channel  $\alpha$  of lead  $\mu$  ( $=L,R$ ) are being scattered into channel  $\alpha'$  of lead  $\mu'$ , whereas the impurity changes its state from  $\beta$  to  $\beta'$ . [In fact, only two types of processes are possible: (a) elastic scatter-

ing, when  $\alpha' = \alpha$ ,  $\beta' = \beta$ , and (b) inelastic scattering, when  $\alpha' = \beta$ ,  $\beta' = \alpha$  ( $\alpha \neq \beta$ )].

$$W_{\mu' \leftarrow \mu}^{\alpha' \beta' \leftarrow \alpha \beta} = \frac{1}{2\pi} \int_{-2t}^{2t} d\epsilon \int_{-2t}^{2t} d\epsilon' f_0(\epsilon) [1 - f_0(\epsilon')] \\ \times |\mathcal{S}_{\mu';\mu}^{\alpha'\beta';\alpha\beta}(\epsilon + V_\mu + \epsilon_\beta)|^2 \delta(\epsilon + V_\mu + \epsilon_\beta - \epsilon' - V_{\mu'} - \epsilon_{\beta'}). \quad (9)$$

Here, we wrote explicitly the dependence of the scattering matrix on the energy of the system QD+incident electron, whereas  $f_0(\epsilon) = 1 / \{1 + \exp[(\epsilon - \epsilon_F) / (k_B T)]\}$  is the Fermi distribution function;  $V_L - V_R = V$  is the bias voltage.

*Level occupation numbers.* The resulting rate equations, describing transitions between different states of the quantum dot, are

$$\frac{d}{dt} P_\beta(t) = \sum_{\beta' \neq \beta} [W^{\beta;\beta'} P_{\beta'}(t) - W^{\beta';\beta} P_\beta(t)], \quad (10)$$

$$W^{\beta;\beta'} = \sum_{\mu,\mu'} \sum_{\alpha,\alpha'} W_{\mu;\mu'}^{\alpha\beta;\alpha'\beta'} = \sum_{\mu,\mu'} W_{\mu;\mu'}^{\beta\beta';\beta\beta}, \quad \beta \neq \beta', \quad (11)$$

where  $P_\beta(t)$  is the probability that the electron occupying the quantum dot is in the state with energy  $\epsilon_\beta$ . In a stationary state, the occupation numbers  $P_\beta$  can be calculated from equations

$$\frac{d}{dt} P_\beta(t) = 0 \quad (12)$$

supplemented by the normalization condition for the total number of electrons occupying the dot.

$$\sum_{\beta} P_\beta = 1. \quad (13)$$

*Current.* The lead-to-lead current is given by  $I = I_{coh} + I_{incoh}$  as follows:

$$I_{coh} = \sum_{\alpha,\beta} P_\beta (W_{RL}^{\alpha\beta;\alpha\beta} - W_{LR}^{\alpha\beta;\alpha\beta}), \quad (14a)$$

$$I_{incoh} = \sum_{\alpha,\beta} P_\beta (W_{RL}^{\alpha\beta;\beta\alpha} - W_{LR}^{\alpha\beta;\beta\alpha}), \quad (14b)$$

where we have explicitly separated the elastic and inelastic contributions.

The differential conductance is defined as

$$G(V, \phi_{AB}) = \frac{\partial I(V, \phi_{AB})}{\partial V}, \quad (15)$$

where  $\phi_{AB} = 2\pi\Phi / \Phi_0$  is the Aharonov-Bohm phase (proportional to the magnetic flux,  $\Phi$ , divided by the magnetic flux quantum,  $\Phi_0 \equiv hc/e$ ).

## III. RESULTS

We provide results obtained from the above equations for an interferometer that has three levels in the interacting

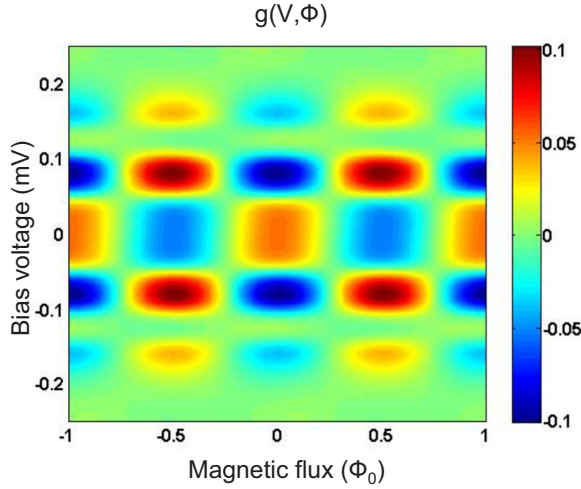


FIG. 2. (Color online) Normalized oscillating part of the differential conductance, Eq. (16), as a function of magnetic flux and bias voltage for the set of parameters appearing in Appendix C. The conductance maximum as a function of flux, as zero bias, becomes a minimum and then a maximum again, as bias is increased.

quantum dot. For the sake of clarity, we chose  $\epsilon_3 - \epsilon_2 = 2(\epsilon_2 - \epsilon_1)$ , so that inelastic cotunneling processes involving levels 1 and 2 begin at lower bias than the cotunneling processes that involve levels 2 and 3. The couplings of the levels to the leads increase with their energies:  $\Gamma_2/\Gamma_1 \approx 3.2$  and  $\Gamma_3/\Gamma_1 \approx 9$ . The complete set of parameters appear in Appendix C.

Our main result is Fig. 2, which shows a plot of the oscillating component of the differential conductance as a function of the magnetic flux through the AB ring (horizontal axis) and the bias voltage applied to the interferometer (vertical axis). For comparison with the experimental results, we normalized the conductance in the same way as in Ref. 10, i.e., the quantity shown is

$$g(V, \phi_{AB}) = \frac{G(V, \phi_{AB}) - G_{mean}(V)}{G_{mean}(V)}, \quad (16)$$

where  $G_{mean}(V)$  is the differential conductance averaged over the period of the magnetic flux,  $\phi_{AB}$ . Comparing this figure to Fig. 3 of the experiment by Sigrist *et al.*,<sup>10</sup> we observe the same characteristic features: (i) depending on the bias voltage, AB oscillations of the differential conductance may have maximum or minimum at zero magnetic flux; (ii) the amplitude of the conductance oscillations relative to the nonoscillating background decreases with increasing bias; and (iii) the number of switching events (i.e., instances when conductance AB oscillations change from maximum at  $\phi_{AB} = 0$  to minimum or vice versa) is not equal to the number of inelastic onsets (in the case at hand, we have four switchings, but only three inelastic onsets, corresponding to  $\epsilon_2 - \epsilon_1$ ,  $\epsilon_3 - \epsilon_2$ , and  $\epsilon_3 - \epsilon_1$ , respectively). Let us discuss these features in greater detail.

The mean value and the oscillating component (at zero magnetic flux) of the differential conductance as functions of bias are shown in Figs. 3 and 4, respectively. In Fig. 3, one can see clearly the three inelastic onsets, that is, three sharp

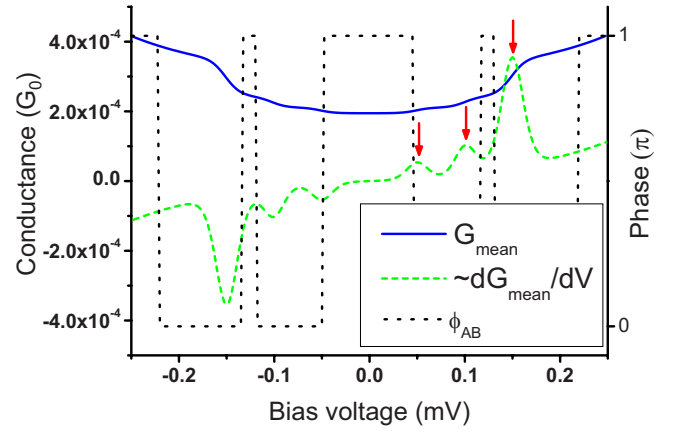


FIG. 3. (Color online) Differential conductance (solid blue), its derivative (dash green), and AB phase of conductance oscillations as functions of bias voltage (dotted black). The onset of the inelastic processes, corresponding to  $V = \epsilon_j - \epsilon_i$  (arrows), is evident.

increases of conductance at bias voltage equal to spacing between any two of the three levels in the system (arrows corresponding to  $V = \epsilon_i - \epsilon_j$ ). For clarity, we show on the same plot the first derivative of the conductance and the phase of conductance oscillations (both multiplied by constant factors). The phase is defined as the sign of the AB oscillations relative to  $G_{mean}$ , i.e., it is  $\pi$  if the oscillations have maximum around zero magnetic flux and 0 otherwise. It is necessary to point out that at finite bias the Onsager–Büttiker symmetries for a two-terminal structure do not require that the phase should be restricted to 0,  $\pi$ ;<sup>5</sup> therefore, our definition of phase is not mathematically strict. Nevertheless, for the set of parameters used here (see Fig. 2) an extremum is found at zero phase even at finite voltage.

The oscillating component of the conductance (Fig. 4) changes its sign four times. The first change occurs when the bias reaches value  $V = \epsilon_2 - \epsilon_1$ , i.e., when inelastic cotunneling process becomes possible, in which case an electron occupying level 1 leaves the dot, whereas another electron can enter the dot and occupies level 2. While such processes do not

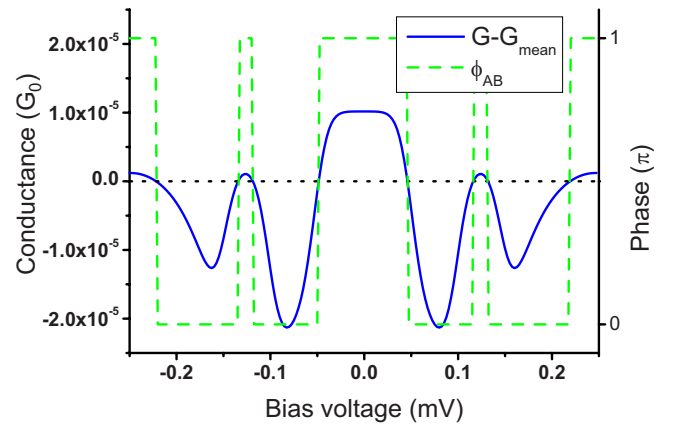


FIG. 4. (Color online) The oscillating contribution to the differential conductance at zero field (solid blue) and AB phase of conductance oscillations (dash green) as a function of bias voltage.

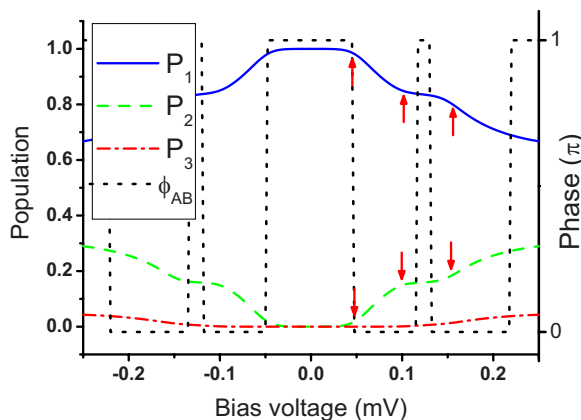


FIG. 5. (Color online) Populations of QD levels as functions of bias voltage. With increasing voltage and with the onset of inelastic processes (arrows), there is a significant change in the relative occupations of the different levels.

contribute to the coherent AB oscillations (they change the state of the dot, thus leaving “trace in the environment”),<sup>17</sup> they play an important role in changing the occupation of the different levels of the dot. In particular, population of level 2, which was for small bias occupied only due to finite temperature, increases, as can be seen in Fig. 5, where we show how the populations of all three levels in the interacting arm of the interferometer depend on the applied bias (at  $\phi_{AB}=0$ ). AB oscillations of conductance result from elastic cotunneling processes, in which electron can tunnel through any of the dot levels. The relative weights of these processes are proportional to the probability for the respective level to be occupied, and therefore for low bias all tunneling processes are suppressed, except those that happen via level 1 or via intermediate state in which the dot is occupied by two electrons (the latter will be suppressed, if the Coulomb interaction is large). Thus, the increase of the occupation of level 2 enhances the weight of the corresponding elastic cotunneling processes, whose contribution to AB oscillations has phase opposite to that of level 1 (due to the opposite parity of these two levels). Due to stronger coupling of level 2 to the leads, the oscillations of opposite phase eventually outweigh those due to level 1 and phase switching occurs.

This interplay between the level coupling strength and its population leads to some interesting effects that happen when the bias is further increased. At the second inelastic onset, i.e., when  $V=\epsilon_3-\epsilon_2$ , occupation of level 3 starts to grow due to transitions from level 2. However, the bias is still not high enough to excite electrons from level 1 to level 3 directly; therefore, level 3 is still being intensively depopulated by transitions to level 1, which results in simultaneous increasing of the population of levels 1 and 3, and saturation (or even a decrease) of the population of level 2. Therefore, the second switching of AB phase occurs due to the change in the relative populations of levels 1 and 2. It is necessary to stress the role of the coupling strengths on the population redistribution: For low temperatures, the population of level 3 may be extremely small, but the switching still occurs since level 2 is effectively depopulated by transitions to level 1 via level 3.

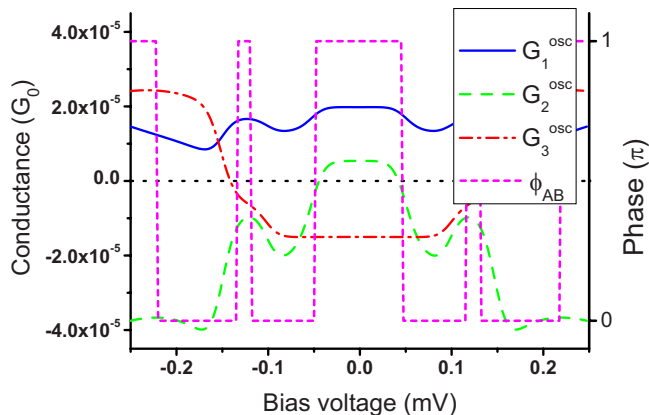


FIG. 6. (Color online) Contributions of different levels in AB oscillations as functions of bias at zero magnetic flux.

Further increase of the bias leads to increase of the population of level 2, which again outweighs that of levels 1 and 3 and causes the third switching. Finally, at the biases greater than  $\epsilon_3-\epsilon_1$ , direct population of level 3 from the lowest energy level 1 starts and the contribution of transport with level 3 occupied eventually takes over all other contributions and results in the fourth switching occurrence.

The contributions of different levels to the AB oscillations are shown in Fig. 6. Let us also point out that a contribution of a level to AB oscillations may not always have the same sign. Thus, there is a regime in which two levels of different parities (levels 2 and 3) give the same sign contribution to AB oscillations. The reason for that is finite value of Coulomb interaction, which allows for two cotunneling processes: (a) hole tunneling via the occupied level (with intermediate state being an empty dot), and (b) electron tunneling via an unoccupied level (with intermediate state being the dot twice occupied). These two processes have energy denominators of different signs. In other words, the former process involves exchanging the two electrons and therefore contributes with the sign different from the latter process. Thus, for example, the contribution of level 3 to the AB oscillations is negative as long as this level is unoccupied, but it becomes positive when the population of this level becomes nonzero. This change of sign does not occur in the limit of large Coulomb interaction, when only hole tunneling (or only electron tunneling) is possible.

Coherent (elastic cotunneling) and incoherent (inelastic cotunneling) contributions to the conductance are depicted in Fig. 7. Inelastic cotunneling never contributes to AB oscillations and therefore presents a background, reducing visibility of the oscillations. The contribution due to the elastic processes contains both oscillating and constant (“elastic background”) components, whose relative size depends on the relative transmission of the two arms of the interferometer. The elastic background is minimized when the transmissions through the two arms of the devices are of the same order.

So far, we have considered the system of levels with strictly alternating parity, Fig. 8(a). However, the effect of redistribution of the dot population between different levels, considered above, can manifest itself in an interesting way also in cases when the parity of the levels is not strictly

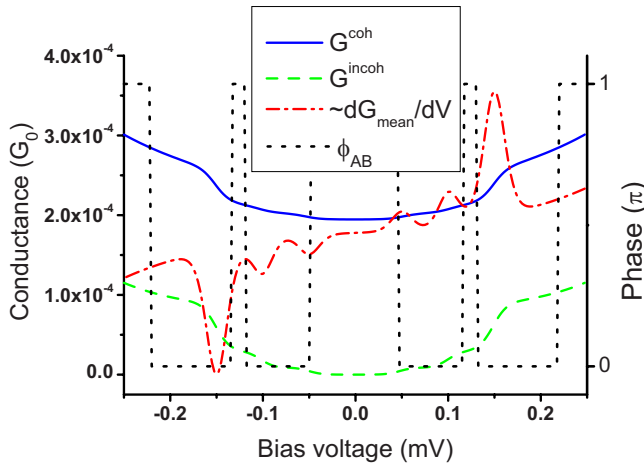


FIG. 7. (Color online) Coherent (elastic cotunneling) and incoherent (inelastic cotunneling) contributions to the differential conductance (shown, respectively, in solid blue and dashed green).

alternating, e.g., the case shown in Fig. 8(b), where level 3 has the same parity as level 2. The oscillating contribution to the differential conductance of such a system is shown in Fig. 9, where the calculations were done with the parameters used above, except the Coulomb interaction, which was taken to be 2.4 times bigger. In addition to the first conductance switch (which occur when inelastic cotunneling with participation of level 2 begins), there are two more switching events which appear after the second and third inelastic onsets (i.e., when level 3 starts being populated from level 2 and slows populating of the latter, and when level 3 starts to be populated directly from level 1).

Thus, the switching mechanism proposed in this paper has rather moderate demands in respect to the statistics of level parity in a quantum dot.

One may try to explain the results of Ref. 10 as originating from electrostatic AB effect.<sup>12</sup> Indeed, due to their small transmission, the quantum dots can be thought of as barriers embedded in the two arms of the interferometer, the whole device thus being an implementation of the proposal for measuring electrostatic AB effect made by Nazarov<sup>11</sup> and van der Wiel *et al.*<sup>12</sup> The main distinction between the electrostatic AB effect and the scenario described in this paper are the intervals between switchings. In electrostatic AB effect, the switchings have to occur with a certain bias voltage period, determined by the electron time of flight through the

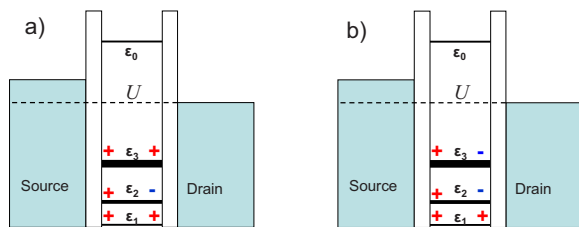


FIG. 8. (Color online) Energy diagrams for the two cases considered: (a) strictly alternating parity of levels, and (b) levels 2 and 3 having the same parity.

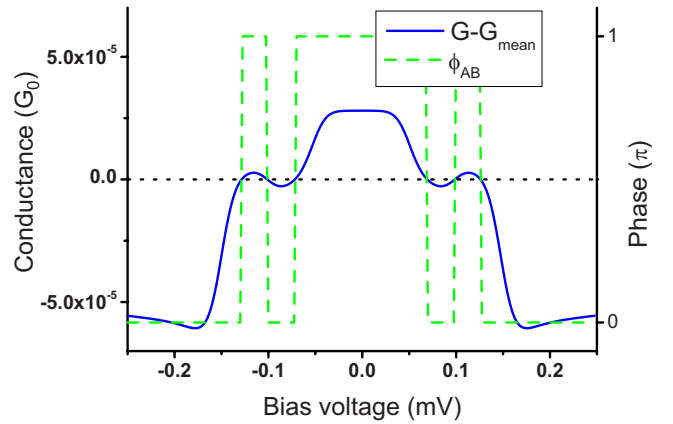


FIG. 9. (Color online) The oscillating contribution to the differential conductance (solid blue) and AB phase of conductance oscillations (dash green) as functions of bias voltage in the case when the parity of levels is not strictly alternating [Fig. 8(b)].

interferometer. This means that switching events have to be separated by approximately equal bias voltage intervals (the period varying to the extent that the density of states depends on energy). On the other hand, the mechanism proposed in this paper allows for the switchings to be separated by unequal bias intervals, as indeed is the case in the experiment.<sup>10</sup> Moreover, the first switching is clearly correlated with the onset of inelastic cotunneling, which cannot be the case for electrostatic AB effect. Experimentally, these two mechanisms can be compared by studying interferometers with the same size of quantum dots but different lengths of the arms, i.e., different periods of electrostatic AB oscillations.

Another important way to distinguish between the two possible explanations is by observing the characteristic behavior of the phase of AB oscillations as it changes between 0 and  $\pi$ . In electrostatic AB effect, this change is smooth, almost linear in bias,<sup>12,18</sup> whereas in the experiment by Sigrist *et al.*, the phase is almost constant, except when the bias is close to its switching value, in which case the phase flows rapidly between 0 and  $\pi$ . The latter phase behavior can be reproduced within the switching mechanism proposed in this paper. However, it requires application of many-body scattering theory and cannot be done within the one-particle scattering matrix approach employed above, as it incorrectly describes phase behavior at small bias. Therefore, we leave the discussion of these interesting phase phenomena to another publication.<sup>19</sup>

#### IV. CONCLUSIONS

We have addressed the findings of the experiment by Sigrist *et al.*<sup>10</sup> We have shown that switching of the phase of the AB oscillations of the conductance between 0 and  $\pi$  as a function of bias can be explained as the result of transport through the interacting arm of the interferometer being dominated at different biases by quantum dot states of different parities.

The number of switching events is not necessarily equal to the number of levels in the interacting arm, which agrees

with experiment and finds its explanation in complex redistribution of electron population between different levels. In particular, the number of switching events may exceed the number of level parity changes in the bias window (even when the parity of the levels is not strictly alternating).

Finally, the correlation between the first switching of the phase and the onset of the inelastic cotunneling, as well as unequal separation of the biases at which the switching occurs, give reason to think that our explanation of the experiment is preferable to the one based on electrostatic AB effect.<sup>11,12</sup>

### ACKNOWLEDGMENTS

The authors would like to thank T. Ihn for sharing with us details of the experimental work. We also thank V. Kashcheyevs and T. Aono for many useful discussions. This work was supported in part by the ISF and BSF.

### APPENDIX A: SCHRIEFFER-WOLFF TRANSFORMATION FOR A QUANTUM DOT INSERTED IN A TIGHT-BINDING CHAIN

Let us consider the following Hamiltonian, describing a QD sandwiched between two leads, where each level of the dot is coupled to a separate channel in the leads. The channels in the leads are assumed to be identical, whereas the states in the dot have different energies:

$$H = H_L + H_R + H_D + H_T, \quad (\text{A1})$$

$$H_D = \sum_{\alpha} \epsilon_{\alpha} n_{\alpha} + \frac{U}{2} \sum_{\alpha, \beta \neq \alpha} n_{\alpha} n_{\beta} \quad (n_{\alpha} = d_{\alpha}^{\dagger} d_{\alpha}), \quad (\text{A2a})$$

$$H_L = -t \sum_{\alpha, j=-\infty}^{-1} (c_{\alpha, j-1}^{\dagger} c_{\alpha, j} + c_{\alpha, j}^{\dagger} c_{\alpha, j-1}) + V_L \sum_{\alpha, j=-\infty}^{-1} c_{\alpha, j}^{\dagger} c_{\alpha, j}, \quad (\text{A2b})$$

$$H_R = -t \sum_{\alpha, j=1}^{+\infty} (c_{\alpha, j+1}^{\dagger} c_{\alpha, j} + c_{\alpha, j}^{\dagger} c_{\alpha, j+1}) + V_R \sum_{\alpha, j=1}^{+\infty} c_{\alpha, j}^{\dagger} c_{\alpha, j}, \quad (\text{A2c})$$

$$H_T = \sum_{\alpha} (t_{L\alpha} d_{\alpha}^{\dagger} c_{\alpha, -1} + t_{L\alpha}^* c_{\alpha, -1}^{\dagger} d_{\alpha} + t_{R\alpha} d_{\alpha}^{\dagger} c_{\alpha, 1} + t_{R\alpha}^* c_{\alpha, 1}^{\dagger} d_{\alpha}). \quad (\text{A2d})$$

In order to perform Schrieffer–Wolff (SW) transformation,<sup>14</sup> we first transform the lead Hamiltonians to the representation, in which they are diagonal,

$$c_{R\alpha k} = \sum_{n=1}^{+\infty} \phi_k(n) c_{\alpha, n}, \quad c_{L\alpha k} = \sum_{n=-\infty}^{-1} \phi_k(n) c_{\alpha, n},$$

$$\phi_k(n) = \sqrt{\frac{2}{\pi}} \sin(kn). \quad (\text{A3})$$

The reciprocal relations are

$$c_{\alpha, n} = \int_0^{\pi} dk \phi_k(n) c_{R\alpha k} \quad \text{if } n \geq 1;$$

$$c_{\alpha, n} = \int_0^{\pi} dk \phi_k(n) c_{L\alpha k} \quad \text{if } n \leq -1. \quad (\text{A4})$$

The lead Hamiltonians take form

$$H_L = \sum_{\alpha} \int_0^{\pi} dk (\epsilon_k + V_L) c_{L\alpha k}^{\dagger} c_{L\alpha k},$$

$$H_R = \sum_{\alpha} \int_0^{\pi} dk (\epsilon_k + V_R) c_{R\alpha k}^{\dagger} c_{R\alpha k}, \quad (\text{A5})$$

where

$$\epsilon_k = -2t \cos(k) \quad (\text{A6})$$

is the kinetic energy of electron with quantum number  $k$ .

Now the tunneling Hamiltonian takes form

$$H_T = \sum_{\alpha} \int_0^{\pi} dk [t_{L\alpha} \phi_k(-1) d_{\alpha}^{\dagger} c_{L\alpha k} + t_{L\alpha}^* \phi_k(-1) c_{L\alpha k}^{\dagger} d_{\alpha} + t_{R\alpha} \phi_k(1) d_{\alpha}^{\dagger} c_{R\alpha k} + t_{R\alpha}^* \phi_k(1) c_{R\alpha k}^{\dagger} d_{\alpha}]. \quad (\text{A7})$$

In order to perform the SW transformation, we need to find an operator  $S$  that satisfies the equation

$$H_T + [S, H_L + H_R + H_D] = 0, \quad (\text{A8})$$

then the transformed Hamiltonian will take form

$$\bar{H} = H_L + H_R + H_D + \frac{1}{2}[S, H_T]. \quad (\text{A9})$$

We choose operator  $S$  as

$$S = F - F^{\dagger},$$

$$F = \sum_{\alpha} \int_0^{\pi} dk \left[ A_{R\alpha k} d_{\alpha}^{\dagger} c_{R\alpha k} + \sum_{\beta \neq \alpha} B_{R\alpha k, \beta} n_{\beta} d_{\alpha}^{\dagger} c_{R\alpha k} + A_{L\alpha k} d_{\alpha}^{\dagger} c_{L\alpha k} + \sum_{\beta \neq \alpha} B_{L\alpha k, \beta} n_{\beta} d_{\alpha}^{\dagger} c_{L\alpha k} \right]. \quad (\text{A10})$$

This operator is sufficient in the case when the number of channels is two. For a greater number of channels, it is necessary to add terms that account for the QD being occupied by two, three, and more electrons. However, we neglect such a possibility and consider only single electron entering or leaving dot. In mathematical terms, this is equivalent to performing SW transformation on a restricted basis, which includes only the states with zero, one, and two electrons in the dot.

Now, it is straightforward to show that the coefficients  $A$  and  $B$  should have forms

$$A_{R\alpha k} = \frac{t_{R\alpha} \phi_k(1)}{\epsilon_{\alpha} - \epsilon_k - V_R}, \quad A_{L\alpha k} = \frac{t_{L\alpha} \phi_k(-1)}{\epsilon_{\alpha} - \epsilon_k - V_L},$$

$$B_{R\alpha k, \beta} = t_{R\alpha} \phi_k(1) \left( \frac{1}{\epsilon_{\alpha} + U - \epsilon_k - V_R} - \frac{1}{\epsilon_{\alpha} - \epsilon_k - V_R} \right),$$

$$B_{L\alpha k, \beta} = t_{L\alpha} \phi_k(-1) \left( \frac{1}{\epsilon_\alpha + U - \epsilon_k - V_L} - \frac{1}{\epsilon_\alpha - \epsilon_k - V_L} \right). \quad (\text{A11})$$

The transformed Hamiltonian is

$$\bar{H} = H_L + H_R + H_D + \sum_{j=1}^6 W_j, \quad (\text{A12})$$

where

$$W_1 = \frac{1}{2} \sum_{\alpha} \int_0^{\pi} dk [A_{R\alpha k} t_{R\alpha}^* \phi_k(1) + A_{L\alpha k} t_{L\alpha}^* \phi_k(-1) + A_{R\alpha k}^* t_{R\alpha} \phi_k(1) + A_{L\alpha k}^* t_{L\alpha} \phi_k(-1)] n_{\alpha} = \sum_{\alpha} \Delta \epsilon_{\alpha} n_{\alpha} \quad (\text{A13})$$

describes the correction to the dot energies due to coupling to the leads. In the following, we will neglect this term—the appropriate corrections can be included in energies  $\epsilon_{\alpha}$  of the Hamiltonian  $H_D$ .

$$W_2 = - \sum_{\alpha} (v_{rr}^{\alpha} c_{\alpha,1}^+ c_{\alpha,1} + v_{lr}^{\alpha} c_{\alpha,-1}^+ c_{\alpha,1} + v_{rl}^{\alpha} c_{\alpha,1}^+ c_{\alpha,-1} + v_{ll}^{\alpha} c_{\alpha,-1}^+ c_{\alpha,-1}),$$

$$v_{rr}^{\alpha} \approx \frac{|t_{R\alpha}|^2}{\epsilon_{\alpha} - \epsilon_F - V_R}, \quad v_{ll}^{\alpha} \approx \frac{|t_{L\alpha}|^2}{\epsilon_{\alpha} - \epsilon_F - V_L},$$

$$v_{lr}^{\alpha} = \frac{1}{2} t_{R\alpha} t_{L\alpha}^* \left( \frac{1}{\epsilon_{\alpha} - \epsilon_F - V_R} + \frac{1}{\epsilon_{\alpha} - \epsilon_F - V_L} \right), \quad v_{rl}^{\alpha} = (v_{lr}^{\alpha})^*. \quad (\text{A14})$$

$W_2$  describes elastic cotunneling through the QD without account for interactions. Following SW, we replaced in the denominators electron kinetic energy,  $\epsilon_k$ , by the Fermi energy. It is essential to keep in mind that, since the leads are kept at different biases, their chemical potentials are different:  $\mu_L = \epsilon_F + V_L$ ,  $\mu_R = \epsilon_F + V_R$ .

$$W_3 = \frac{1}{2} \sum_{\alpha, \beta \neq \alpha} \int_0^{\pi} dk \int_0^{\pi} dk' [B_{R\alpha k, \beta} t_{R\beta}^* \phi_{k'}(1) d_{\beta}^+ d_{\alpha}^+ c_{R\alpha k} c_{R\beta k'} + B_{R\alpha k, \beta} t_{L\beta}^* \phi_{k'}(-1) d_{\beta}^+ d_{\alpha}^+ c_{R\alpha k} c_{L\beta k'} + B_{L\alpha k, \beta} t_{R\beta}^* \phi_{k'}(1) d_{\beta}^+ d_{\alpha}^+ c_{L\alpha k} c_{R\beta k'} + B_{L\alpha k, \beta} t_{L\beta}^* \phi_{k'}(1) d_{\beta}^+ d_{\alpha}^+ c_{L\alpha k} c_{L\beta k'} + \text{H.c.}]. \quad (\text{A15})$$

$W_3$  describes simultaneous tunneling of two electrons into or out of the dot. In the following, we neglect this term, since the corresponding processes are energetically unavailable.

$$W_4 = \sum_{\alpha, \beta \neq \alpha} [v_{rr}^{\beta\alpha} c_{\beta,1}^+ d_{\alpha}^+ d_{\beta} c_{\alpha,1} + v_{lr}^{\beta\alpha} c_{\beta,-1}^+ d_{\alpha}^+ d_{\beta} c_{\alpha,1} + v_{rl}^{\beta\alpha} c_{\beta,1}^+ d_{\alpha}^+ d_{\beta} c_{\alpha,-1} + v_{ll}^{\beta\alpha} c_{\beta,-1}^+ d_{\alpha}^+ d_{\beta} c_{\alpha,-1}],$$

$$v_{rr}^{\beta\alpha} = \frac{1}{2} t_{R\alpha} t_{R\beta}^* \left( \frac{1}{\epsilon_{\alpha} + U - \epsilon_F - V_R} - \frac{1}{\epsilon_{\alpha} - \epsilon_F - V_R} + \frac{1}{\epsilon_{\beta} + U - \epsilon_F - V_R} - \frac{1}{\epsilon_{\beta} - \epsilon_F - V_R} \right),$$

$$v_{ll}^{\beta\alpha} = \frac{1}{2} t_{L\alpha} t_{L\beta}^* \left( \frac{1}{\epsilon_{\alpha} + U - \epsilon_F - V_L} - \frac{1}{\epsilon_{\alpha} - \epsilon_F - V_L} + \frac{1}{\epsilon_{\beta} + U - \epsilon_F - V_L} - \frac{1}{\epsilon_{\beta} - \epsilon_F - V_L} \right),$$

$$v_{rl}^{\beta\alpha} = \frac{1}{2} t_{L\alpha} t_{R\beta}^* \left( \frac{1}{\epsilon_{\alpha} + U - \epsilon_F - V_L} - \frac{1}{\epsilon_{\alpha} - \epsilon_F - V_L} + \frac{1}{\epsilon_{\beta} + U - \epsilon_F - V_R} - \frac{1}{\epsilon_{\beta} - \epsilon_F - V_R} \right),$$

$$v_{lr}^{\beta\alpha} = (v_{rl}^{\beta\alpha})^*. \quad (\text{A16})$$

$W_4$  describes inelastic cotunneling through the quantum dot, i.e., the tunneling events when the dot changes its state, while the incident electron is transferred from one lead to the other or reflected back.

$$W_5 = \frac{1}{2} \sum_{\alpha, \beta \neq \alpha} \int_0^{\pi} dk [B_{R\alpha k, \beta} t_{R\alpha}^* \phi_k(1) + B_{L\alpha k, \beta} t_{L\alpha}^* \phi_k(-1) + \text{c.c.}] \times n_{\alpha} n_{\beta} = \frac{1}{2} \sum_{\alpha, \beta \neq \alpha} \Delta U_{\alpha\beta} n_{\alpha} n_{\beta}. \quad (\text{A17})$$

$W_5$  describes correction to the Coulomb energy and is expected to be small; in the following, we neglect this term. Finally, we also have

$$W_6 = - \sum_{\alpha, \beta \neq \alpha} (v_{rr}^{\alpha\alpha} n_{\beta} c_{\alpha,1}^+ c_{\alpha,1} + v_{lr}^{\alpha\alpha} n_{\beta} c_{\alpha,-1}^+ c_{\alpha,1} + v_{rl}^{\alpha\alpha} n_{\beta} c_{\alpha,1}^+ c_{\alpha,-1} + v_{ll}^{\alpha\alpha} n_{\beta} c_{\alpha,-1}^+ c_{\alpha,-1}),$$

$$v_{rr}^{\alpha\alpha} = |t_{R\alpha}|^2 \left( \frac{1}{\epsilon_{\alpha} + U - \epsilon_F - V_R} - \frac{1}{\epsilon_{\alpha} - \epsilon_F - V_R} \right),$$

$$v_{ll}^{\alpha\alpha} = |t_{L\alpha}|^2 \left( \frac{1}{\epsilon_{\alpha} + U - \epsilon_F - V_L} - \frac{1}{\epsilon_{\alpha} - \epsilon_F - V_L} \right),$$

$$v_{lr}^{\alpha\alpha} = \frac{1}{2} t_{R\alpha} t_{L\alpha}^* \left( \frac{1}{\epsilon_{\alpha} + U - \epsilon_F - V_R} - \frac{1}{\epsilon_{\alpha} - \epsilon_F - V_R} + \frac{1}{\epsilon_{\alpha} + U - \epsilon_F - V_L} - \frac{1}{\epsilon_{\alpha} - \epsilon_F - V_L} \right),$$

$$v_{rl}^{\alpha\alpha} = (v_{lr}^{\alpha\alpha})^*, \quad (\text{A18})$$

which describes the correction to elastic cotunneling contribution,  $W_2$ , which arises when the dot is occupied by an electron ( $W_2$  is elastic cotunneling through an empty dot: “hole tunneling”).



For the reference arm, in which we neglect the Coulomb interaction, the Schrieffer–Wolff transformation readily produces the only tunneling term

$$\begin{aligned}
W_{ref} = & - \sum_{\alpha} (\omega_{rr} c_{\alpha,1}^+ c_{\alpha,1} + \omega_{lr} c_{\alpha,-1}^+ c_{\alpha,1} + \omega_{rl} c_{\alpha,1}^+ c_{\alpha,-1} \\
& + \omega_{ll} c_{\alpha,-1}^+ c_{\alpha,-1}), \\
\omega_{rr} \approx & \frac{|t_{R,0}|^2}{\epsilon_0 - \epsilon_F - V_R}, \quad \omega_{ll} \approx \frac{|t_{L,0}|^2}{\epsilon_0 - \epsilon_F - V_L}, \\
\omega_{lr} = & \frac{1}{2} t_{R,0} t_{L,0}^* \left( \frac{1}{\epsilon_0 - \epsilon_F - V_R} + \frac{1}{\epsilon_0 - \epsilon_F - V_L} \right), \quad \omega_{rl} = (\omega_{lr})^*,
\end{aligned} \tag{A19}$$

where  $\epsilon_0$  and  $t_{L,0}$ ,  $t_{R,0}$  are the level energy and the tunneling amplitudes for this arm, which we assume to be independent on the channel index.

We neglect  $W_{1,5}$  describing corrections to the coefficients and  $W_3$  describing two-particle tunneling, but keep the terms  $W_{2,4,6}$  which, together with  $H_L$ ,  $H_R$ ,  $H_D$ , and  $W_{ref}$ , form Hamiltonian  $\mathcal{H}$ , Eq. (1), used in this paper. [Let us point out that neither of these operators changes the occupation of the QD. In the cotunneling regime, the QD is occupied by only one electron, which allows us to neglect the Coulomb term in Eq. (A2a).]

## APPENDIX B: SCATTERING MATRIX

Above Kondo temperature Hamiltonian, Eqs. (1) and (2) can be treated as a one-particle Hamiltonian, if we consider the state of the QD as an additional channel index. Thus, the scattering matrix can be determined by directly solving Schrödinger equation (see, e.g., Ref. 4)

$$\mathcal{H}|\Psi\rangle = E|\Psi\rangle, \tag{B1}$$

for one-electron scattering states defined as

$$\begin{aligned}
|\Psi\rangle = & \sum_{\alpha,\beta} \left[ \sum_{n=-\infty}^{-1} (A_L^{\alpha\beta} e^{iq_{\beta}n} + B_L^{\alpha\beta} e^{-iq_{\beta}n}) d_{\beta}^+ c_{\alpha,n}^+ + \sum_{n=1}^{+\infty} (A_R^{\alpha\beta} e^{ik_{\beta}n} \right. \\
& \left. + B_R^{\alpha\beta} e^{-ik_{\beta}n}) d_{\beta}^+ c_{\alpha,n}^+ \right] |0\rangle,
\end{aligned} \tag{B2}$$

where  $|0\rangle$  is the state with no particles. In Eq. (B2),  $A_L^{\alpha\beta}$  ( $B_R^{\alpha\beta}$ ) and  $B_L^{\alpha\beta}$  ( $A_R^{\alpha\beta}$ ) are the amplitudes of the waves, respectively, incident and outgoing from left(right); indices  $\beta$  and  $\alpha$  label, respectively, the state of the QD and the lead channel.

The wave vectors  $q_{\beta}$  and  $k_{\beta}$  are defined as solutions of equations

$$E = \epsilon_{\beta} + V_L - 2t \cos q_{\beta},$$

$$E = \epsilon_{\beta} + V_R - 2t \cos k_{\beta}, \tag{B3}$$

where  $E$  is the total energy of the electron and the QD,  $V_L$  and  $V_R$  are the changes in the potential energy of electrons in the leads, whereas  $\epsilon_k = -2t \cos k$  is the kinetic energy of the electron.

Upon substitution of the wave function, Eq. (B2), into the Schrödinger equation, Eq. (B1), we readily obtain the following equation, which relates the scattering amplitudes and simultaneously defines the amplitude scattering matrix

$$\begin{pmatrix} \mathbf{B}_L \\ \mathbf{A}_R \end{pmatrix} = \hat{S} \begin{pmatrix} \mathbf{A}_L \\ \mathbf{B}_R \end{pmatrix}. \tag{B4}$$

The matrix  $\hat{S}$  in this equations is given by

$$\hat{S} = -\hat{\mathcal{M}}^{-1} \hat{\mathcal{N}}, \tag{B5}$$

where the nonzero elements of matrices  $\hat{\mathcal{M}}$  and  $\hat{\mathcal{N}}$  are given by

$$\hat{\mathcal{M}} = \begin{pmatrix} \hat{\mathcal{M}}_{LL} & \hat{\mathcal{M}}_{LR} \\ \hat{\mathcal{M}}_{RL} & \hat{\mathcal{M}}_{RR} \end{pmatrix}, \quad \hat{\mathcal{N}} = \begin{pmatrix} \hat{\mathcal{N}}_{LL} & \hat{\mathcal{N}}_{LR} \\ \hat{\mathcal{N}}_{RL} & \hat{\mathcal{N}}_{RR} \end{pmatrix}, \tag{B6a}$$

$$\mathcal{M}_{LL}^{\alpha\beta;\alpha\beta} = t - [v_{ll}^{\alpha} + (1 - \delta_{\alpha,\beta}) v_{ll}^{\alpha\alpha}] e^{iq_{\beta}},$$

$$\mathcal{M}_{LL}^{\alpha\beta;\beta\alpha} = (1 - \delta_{\alpha,\beta}) v_{ll}^{\alpha\beta} e^{iq_{\alpha}},$$

$$\mathcal{M}_{LR}^{\alpha\beta;\alpha\beta} = -[v_{lr}^{\alpha} + (1 - \delta_{\alpha,\beta}) v_{ll}^{\alpha\alpha}] e^{ik_{\beta}},$$

$$\mathcal{M}_{LR}^{\alpha\beta;\beta\alpha} = (1 - \delta_{\alpha,\beta}) v_{lr}^{\alpha\beta} e^{ik_{\alpha}},$$

$$\mathcal{M}_{RL}^{\alpha\beta;\alpha\beta} = -[v_{rl}^{\alpha} + (1 - \delta_{\alpha,\beta}) v_{rl}^{\alpha\alpha}] e^{iq_{\beta}},$$

$$\mathcal{M}_{RL}^{\alpha\beta;\beta\alpha} = (1 - \delta_{\alpha,\beta}) v_{rl}^{\alpha\beta} e^{iq_{\alpha}},$$

$$\mathcal{M}_{RR}^{\alpha\beta;\alpha\beta} = t - [v_{rr}^{\alpha} + (1 - \delta_{\alpha,\beta}) v_{rr}^{\alpha\alpha}] e^{ik_{\beta}},$$

$$\mathcal{M}_{RR}^{\alpha\beta;\beta\alpha} = (1 - \delta_{\alpha,\beta}) v_{rr}^{\alpha\beta} e^{ik_{\alpha}}, \tag{B6b}$$

and

$$\mathcal{N}_{LL}^{\alpha\beta;\alpha\beta} = t - [v_{ll}^{\alpha} + (1 - \delta_{\alpha,\beta}) v_{ll}^{\alpha\alpha}] e^{-iq_{\beta}},$$

$$\mathcal{N}_{LL}^{\alpha\beta;\beta\alpha} = (1 - \delta_{\alpha,\beta}) v_{ll}^{\alpha\beta} e^{-iq_{\alpha}},$$

$$\mathcal{N}_{LR}^{\alpha\beta;\alpha\beta} = -[v_{lr}^{\alpha} + (1 - \delta_{\alpha,\beta}) v_{ll}^{\alpha\alpha}] e^{-ik_{\beta}},$$

$$\mathcal{N}_{LR}^{\alpha\beta;\beta\alpha} = (1 - \delta_{\alpha,\beta}) v_{lr}^{\alpha\beta} e^{-ik_{\alpha}},$$

$$\mathcal{N}_{RL}^{\alpha\beta;\alpha\beta} = -[v_{rl}^{\alpha} + (1 - \delta_{\alpha,\beta}) v_{rl}^{\alpha\alpha}] e^{-iq_{\beta}},$$

$$\mathcal{N}_{RL}^{\alpha\beta;\beta\alpha} = (1 - \delta_{\alpha,\beta}) v_{rl}^{\alpha\beta} e^{-iq_{\alpha}},$$

$$\mathcal{N}_{RR}^{\alpha\beta;\alpha\beta} = t - [v_{rr}^{\alpha} + (1 - \delta_{\alpha,\beta}) v_{rr}^{\alpha\alpha}] e^{-ik_{\beta}},$$

$$\mathcal{N}_{RR}^{\alpha\beta;\beta\alpha} = (1 - \delta_{\alpha,\beta}) v_{rr}^{\alpha\beta} e^{-ik_{\alpha}}. \tag{B6c}$$

Given that the number of the lead channels (and QD states) is  $M$ , we have total  $M^2$  different channels in our scattering problem, which means that  $S$  is  $2M^2 \times 2M^2$  matrix.

Finally, in order to normalize the wave function and the scattering matrix to unit incident flux, we multiply  $\hat{S}$  by velocity matrices

$$\hat{S} = \hat{u}^{1/2} \hat{S} \hat{u}^{-1/2}, \quad \hat{u} = \begin{pmatrix} \hat{u}_L & 0 \\ 0 & \hat{u}_R \end{pmatrix}, \quad (\text{B7})$$

where

$$u_L^{\alpha,\beta;\alpha'\beta'} = \delta_{\alpha,\alpha'} \delta_{\beta,\beta'} 2t \sin q_\beta, \\ u_R^{\alpha,\beta;\alpha'\beta'} = \delta_{\alpha,\alpha'} \delta_{\beta,\beta'} 2t \sin k_\beta. \quad (\text{B8})$$

### APPENDIX C: PARAMETERS USED IN THE RESULTS SECTION

The level energies were taken to be  $\epsilon_1 = -0.4$  meV,  $\epsilon_2 = -0.35$  meV, and  $\epsilon_3 = -0.25$  meV; the tunneling amplitudes are  $t_{L,1} = 50$   $\mu\text{eV}$ ,  $t_{L,2} = 88.9$   $\mu\text{eV}$ ,  $t_{L,3} = 150$   $\mu\text{eV}$ ,  $t_{L,1} = 50$   $\mu\text{eV}$ ,  $t_{L,2} = -88.9$   $\mu\text{eV}$ , and  $t_{L,3} = 150$   $\mu\text{eV}$ , which correspond to the level widths  $\Gamma_{L,1} = \Gamma_{R,1} = 0.25$   $\mu\text{eV}$ ,  $\Gamma_{L,2} = \Gamma_{R,2} = 0.79$   $\mu\text{eV}$ , and  $\Gamma_{L,3} = \Gamma_{R,3} = 2.25$   $\mu\text{eV}$  (in tight-bonding picture, level width is defined as  $\Gamma = |t_{\mu,\alpha}|^2/t$ ). The Coulomb interaction is  $U = 5$  meV. The parameters of the reference arm are  $\epsilon_0 = -1$  meV,  $t_{L,0} = t_{R,0} = 200$   $\mu\text{eV}$ , and  $\Gamma_{L,0} = \Gamma_{R,0} = 4$   $\mu\text{eV}$ . The temperature is taken to be  $T = 60$  mK.

- 
- <sup>1</sup>A. Yacoby, M. Heiblum, D. Mahalu, and H. Shtrikman, *Phys. Rev. Lett.* **74**, 4047 (1995); R. Schuster, E. Buks, M. Heiblum, D. Mahalu, V. Umansky, and H. Shtrikman, *Nature (London)* **385**, 427 (1997).
- <sup>2</sup>G. Hackenbroich, *Phys. Rep.* **343**, 463 (2001).
- <sup>3</sup>M. Büttiker, *Phys. Rev. Lett.* **57**, 1761 (1986); A. L. Yeyati and M. Büttiker, *Phys. Rev. B* **52**, R14360 (1995); A. Yacoby, R. Schuster, and M. Heiblum, *ibid.* **53**, 9583 (1996).
- <sup>4</sup>O. Entin-Wohlman, A. Aharony, Y. Imry, Y. Levinson, and A. Schiller, *Phys. Rev. Lett.* **88**, 166801 (2002); A. Aharony, O. Entin-Wohlman, T. Otsuka, S. Katsumoto, H. Aikawa, and K. Kobayashi, *Phys. Rev. B* **73**, 195329 (2006).
- <sup>5</sup>C. Bruder, R. Fazio, and H. Schoeller, *Phys. Rev. Lett.* **76**, 114 (1996).
- <sup>6</sup>Y. Oreg and Y. Gefen, *Phys. Rev. B* **55**, 13726 (1997); R. Baltin and Y. Gefen, *Phys. Rev. Lett.* **83**, 5094 (1999); D. I. Golosov and Y. Gefen, *Phys. Rev. B* **74**, 205316 (2006); *New J. Phys.* **9**, 120 (2007).
- <sup>7</sup>P. G. Silvestrov and Y. Imry, *Phys. Rev. Lett.* **85**, 2565 (2000); *New J. Phys.* **9**, 125 (2007).
- <sup>8</sup>Y. Oreg, *New J. Phys.* **9**, 122 (2007); C. Karrasch, T. Hecht, A. Weichselbaum, Y. Oreg, J. von Delft, and V. Meden, *Phys. Rev. Lett.* **98**, 186802 (2007); *New J. Phys.* **9**, 123 (2007).
- <sup>9</sup>G. Hackenbroich, W. D. Heiss, and H. A. Weidenmüller, *Phys. Rev. Lett.* **79**, 127 (1997); R. Baltin, Y. Gefen, G. Hackenbroich, and H. A. Weidenmüller, *Eur. Phys. J. B* **10**, 119 (1999).
- <sup>10</sup>M. Sigrist, Thomas Ihn, K. Ensslin, M. Reinwald, and W. Wegscheider, *Phys. Rev. Lett.* **98**, 036805 (2007).
- <sup>11</sup>Yu. V. Nazarov, *Phys. Rev. B* **47**, 2768 (1993).
- <sup>12</sup>W. G. van der Wiel, Y. V. Nazarov, S. De Franceschi, T. Fujisawa, J. M. Elzerman, E. W. G. M. Huizeling, S. Tarucha, and L. P. Kouwenhoven, *Phys. Rev. B* **67**, 033307 (2003).
- <sup>13</sup>A. Silva, Y. Oreg, and Y. Gefen, *Phys. Rev. B* **66**, 195316 (2002).
- <sup>14</sup>J. R. Schrieffer and P. A. Wolff, *Phys. Rev.* **149**, 491 (1966).
- <sup>15</sup>V. Kashcheyevs, A. Schiller, A. Aharony, and O. Entin-Wohlman, *Phys. Rev. B* **75**, 115313 (2007).
- <sup>16</sup>O. Parcollet and C. Hooley, *Phys. Rev. B* **66**, 085315 (2002); E. V. Sukhorukov, G. Burkard, and D. Loss, *ibid.* **63**, 125315 (2001).
- <sup>17</sup>A. Stern, Y. Aharonov, and Y. Imry, *Phys. Rev. A* **41**, 3436 (1990).
- <sup>18</sup>R. Leturcq, D. Sanchez, G. Gotz, T. Ihn, K. Ensslin, D. C. Driscoll, and A. C. Gossard, *Phys. Rev. Lett.* **96**, 126801 (2006).
- <sup>19</sup>V. I. Puller and Y. Meir (unpublished).